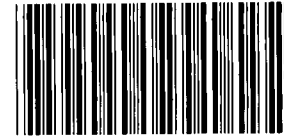


SANDIA REPORT

SAND93-0261 • UC-706
Unlimited Release
Printed March 1993

MICROFICHE

Fiber-Optic Shock Position Sensor



8552864

Jonathan D. Weiss

SANDIA NATIONAL
LABORATORIES
TECHNICAL LIBRARY

Prepared by
Sandia National Laboratories
Albuquerque, New Mexico 87185 and Livermore, California 94550
for the United States Department of Energy
under Contract DE-AC04-76DP00789

Issued by Sandia National Laboratories, operated for the United States Department of Energy by Sandia Corporation.

NOTICE: This report was prepared as an account of work sponsored by an agency of the United States Government. Neither the United States Government nor any agency thereof, nor any of their employees, nor any of their contractors, subcontractors, or their employees, makes any warranty, express or implied, or assumes any legal liability or responsibility for the accuracy, completeness, or usefulness of any information, apparatus, product, or process disclosed, or represents that its use would not infringe privately owned rights. Reference herein to any specific commercial product, process, or service by trade name, trademark, manufacturer, or otherwise, does not necessarily constitute or imply its endorsement, recommendation, or favoring by the United States Government, any agency thereof or any of their contractors or subcontractors. The views and opinions expressed herein do not necessarily state or reflect those of the United States Government, any agency thereof or any of their contractors.

Printed in the United States of America. This report has been reproduced directly from the best available copy.

Available to DOE and DOE contractors from
Office of Scientific and Technical Information
PO Box 62
Oak Ridge, TN 37831

Prices available from (615) 576-8401, FTS 626-8401

Available to the public from
National Technical Information Service
US Department of Commerce
5285 Port Royal Rd
Springfield, VA 22161

NTIS price codes
Printed copy: A03
Microfiche copy: A01

Fiber-Optic Shock Position Sensor*

Jonathan D. Weiss
Test Planning & Diagnostics Department
Sandia National Laboratories
Albuquerque, NM 87185

Abstract

This report describes work performed with FY92 Laboratory Directed Research and Development (LDRD) funding for the development of a fiber-optic shock position sensor used to measure the location of a shock front in the neighborhood of a nuclear explosion. Such a measurement would provide a hydrodynamic determination of nuclear yield. The original proposal was prompted by the Defense Nuclear Agency's interest in replacing as many electrical sensors as possible with their optical counterparts for the verification of a treaty limiting the yield of a nuclear device used in underground testing. Immunity to electromagnetic pulse is the reason for the agency's interest; unlike electrical sensors and their associated cabling, fiber-optic systems do not transmit to the outside world noise pulses from the device containing secret information.

*The original proposal was entitled "Fiber-Optic Shock Velocity Sensor," but the current title is more accurate.

Acknowledgments

I wish to thank Salvador S. Lopez of the Test Planning and Diagnostics Department at Sandia National Laboratories for his essential technical assistance throughout the entire experimental phase of this research. My thanks also to Richard Saxton of Sandia's Explosive Dynamics Laboratory for his expertise in connection with the explosives aspects of this work.

Contents

Introduction	7
Fiber-Optic Shock Position Sensor.....	8
Original Proposal.....	8
Multiloop Sensor	9
Intensity Interferometric Sensor.....	12
Embedded Grating Sensor.....	15
References	17

Figures

1 Configuration for hydrodynamic yield measurement	7
2 Original proposal for shock position sensor	8
3 Detector output vs. time	8
4 Fiber-optic sensor output.....	9
5 Multiloop shock position sensor.....	9
6 Explosives test arrangement for multiloop sensor	10
7 Six-loop sensor using modulated optical source	10
8 Six-loop sensor using steady optical source	11
9 One hundred-loop sensor using steady optical source	11
10 Intensity interferometric sensor	13
11 End reflections using a steady optical source	13
12 End reflections using a modulated optical source.....	14
13 Embedded grating sensor.....	15
14 Two-surface reflection	15
15 Composite reflectivity.....	16
16 Elemental reflectivity	17

Fiber-Optic Shock Position Sensor

Introduction

Many years ago, R. C. Bass and A. J. Chabai of Sandia National Laboratories developed an empirical relationship between the radius of the ground shock front caused by an underground nuclear explosion and time in the region of "strong shock" propagation.¹ This relationship, which has come to be known as the "universal yield relation," is as follows:

$$R/W^{1/3} = A(T/W^{1/3})^B, \quad (1)$$

where W is the explosive yield in kilotons, R is the radius from the explosive center in meters, T is the time relative to zero time in milliseconds, and A and B are constants. The common geological materials encountered in underground testing are:¹

$$A = 6.29 ; B = 0.475 . \quad (2)$$

In the region of "strong shock" propagation, the shock pressure is so high that the material strength of the medium through which it passes is largely irrelevant. Since the material behaves essentially like a fluid, this region close to the device is referred to as hydrodynamic, where the shock pressure is greater

than approximately 55 kilobars.¹ Such pressures exist to about 30 meters from the center of explosion of a 125-kiloton nuclear device in the usual geologic materials. In addition to an upper radius beyond which the pressure is too low for Eq. (1) to be valid, there also exists a lower radius within which the shock no longer appears to be emerging from a point source. In this region, details of the source geometry and support structure significantly perturb the sphericity of the shock front, and Eq. (1) is again invalid. This near region extends to a few meters from the device.

Equation (1) is the basis for a hydrodynamic determination of nuclear yield, as part of the verification of a treaty to limit the yield of such a device used in underground nuclear testing. The geometry of this measurement is illustrated in Figure 1, though obviously not to scale.² Although electrical systems such as the SLIFER and the CORRTX have served as shock position sensors, they are susceptible to electromagnetic pulse (EMP). In particular, the coaxial cable from which they are constructed can detect the timing between certain noise pulses created by the device and transmit that secret information to the outside world. Optical fibers possess no such susceptibility and would thus provide the security required in such a high EMP environment.

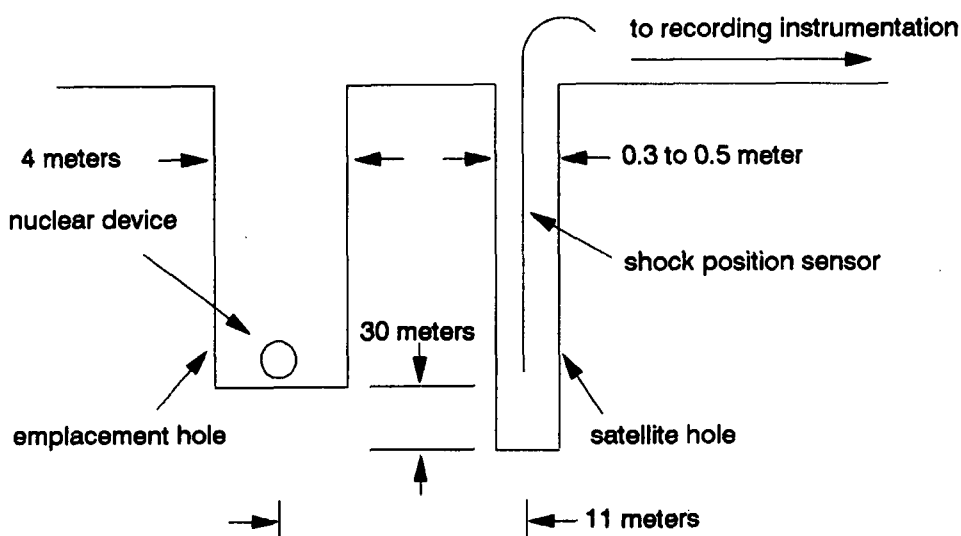


Figure 1. Configuration for hydrodynamic yield measurement

Fiber-Optic Shock Position Sensor

In this section we will describe various concepts for the shock position sensor that were explored, tested, or both. One such concept arose fortuitously during this research. In all cases, our object was to incorporate a large array (~100) of time-of-arrival points compactly into one sensor and record the output on a single data channel. Achieving this goal would result in an essentially quasi-continuous measure of shock position with a minimum of recording capacity.

Original Proposal

Our original proposal for a shock position sensor, shown in Figure 2, consisted of two optical fibers: a multiple-looped one emerging from the optical source and a straight fiber leading to the detector. These two fibers were to be fused to each other at each loop in a manner similar to that used in the construction of multimode fiber-optic couplers. In this way, a small fraction (~1%) of the light from the source fiber would be coupled to the detector fiber at each fusion point, resulting in a detector output that monotonically increases with the number of fusion points. As the shock progresses in the direction indicated, each fusion point would be successively destroyed and the ideal detector output would drop in a staircase fashion (Figure 3). Since the geometry of manufacture and deployment would be known a priori, and the transition times would have been measured, the position of the shock front could be determined at any instant to within one fusion length. These fusion points need not be equally spaced. If greater spatial resolution were needed in certain regions than in others, they could be more densely packed where required.

In contrast to Figure 3 is Figure 4, which is a calculation of the idealized output of a 20-point sensor deployed as in Figure 1 to detect the ground shock created by a 125-kiloton device. The bottom of this sensor is assumed to be at the same depth as the nuclear device, and is 28.5 meters long. This length, combined with the lateral separation of 11 meters, causes the top of the sensor to be 30 meters from the device. The nature of the response in this figure is a consequence of Eq. (1) and the changing orientation of the sensor with respect to the shock propagation direction.

In describing the operation of the sensor, we have ignored recoupling back into the source fiber from the detector fiber. However, during manufacture, the detector output would be monitored as fusion points are added, and adjustments could be made empirically in the degree of coupling at any such point to produce the desired upward staircase response. Thus, the underlying complexity causing this response need not be accounted for explicitly while this sensor is being fabricated. In operation, the destruction of this sensor would simply "walk" (actually "run") the detector output back down the stairs.

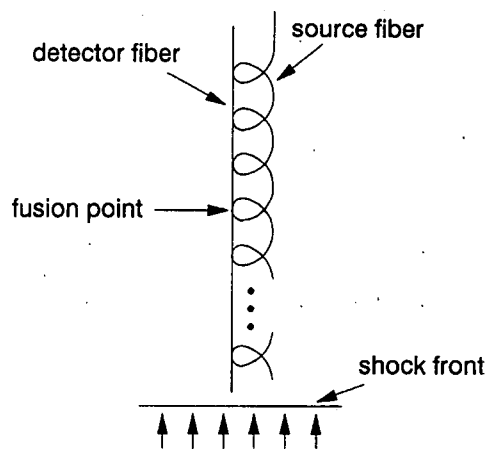


Figure 2. Original proposal for shock position sensor

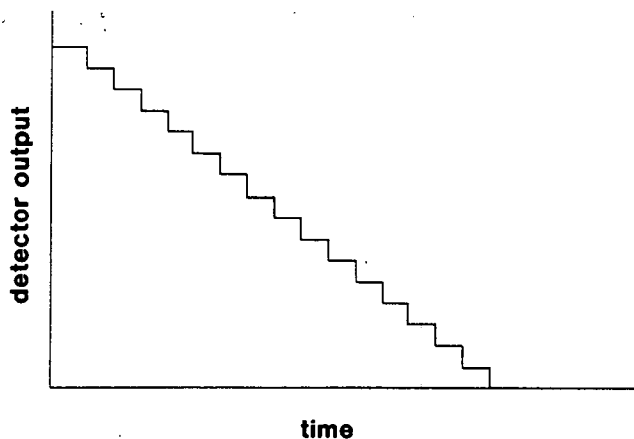


Figure 3. Detector output vs. time

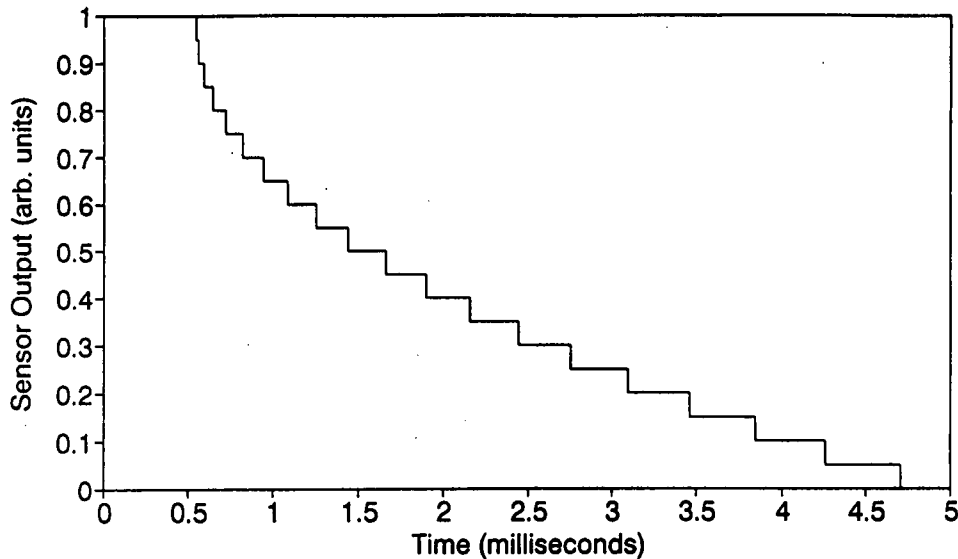


Figure 4. Fiber-optic sensor output (device yield = 125 kilotons)

Multiloop Sensor

The prospective manufacturer of this device, Canada Wire & Cable Ltd., Canstar Division, normally fabricates fiber-optic splitters with a minimum 7% coupling ratio—that is, a minimum of 7% would be transmitted from one fiber to another at any one of the fusion points described above. A coupling ratio of only 1% would be too unstable with temperature to guarantee successful operation. For this and various manufacturing reasons, we agreed that this sensor would not be fabricated. However, a multiloop sensor that could perform the same measurement was manufactured and successfully tested. This device, illustrated in Figure 5, consists of two 8×100 conventional fiber-optic couplers and 100 loops of optical fiber connected between them. Any one of the first set of eight fibers could be connected to its own remotely located optical source through a lead fiber (not shown but extending off to the right of the figure). Similar lead fibers emanating from the other set are bundled together and connected to a remote photodetector with a face large enough to accommodate all eight of them. Light from each source fiber is divided roughly uniformly among all 100 fiber loops, and light leaving each loop is similarly divided among the eight detector fibers. However, since 92 of the potential 100 output fibers are dead-ended within the coupler, only 8% of the optical power entering this second coupler can reach the detector.

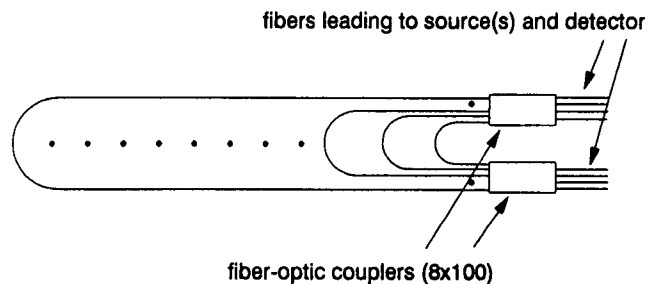


Figure 5. Multiloop shock position sensor

The operation of this sensor is similar to the one originally proposed: when the shock wave reaches each loop, it breaks and produces a small drop in the optical power reaching the detector. The result is a downward staircase output similar to the one shown in Figure 3.

In principle, one could use two 100×100 couplers with a potential of connecting them to 100 different optical sources and of recovering all the output power, as opposed to only 8%. This would result in a much larger signal, but it may be impractical because of the resources required to produce it. Two hundred lead fibers connecting this sensor to the detector and 100 sources is an extremely large number of both kinds of components to dedicate to one measurement. In addition, a detector large enough to accommodate 100 fibers might have too low a frequency response, unless

the fibers were butt-coupled right to the detector face. Nevertheless, the choice of 8×100 couplers is not unique; in our case, it was made because eight-fiber cables are typically, though not exclusively, available at the Nevada Test Site.

Although the operation of this sensor seemed extremely straightforward, ever mindful of the "Law of Maximum Perversity of the Universe," we decided first to test a homemade, six-loop device. This was to be an inexpensive way of correcting unanticipated problems. We had originally intended not to use a steady laser-diode source for these tests but, rather, one modulated at 80 mHz. The sensor would then amplitude-modulate this carrier and the detector would be tuned to frequencies of ~ 80 mHz. We had used such a scheme in the past to enhance the rejection of unwanted optical signals provided by narrow-band optical filtering. In this case, we anticipated that such a signal would most likely be shock-induced luminescence with temporal frequencies well below 80 mHz.

The basic explosives arrangement for these experiments is illustrated in Figure 6, where a length of detonation cord (or Primacord), manufactured by the Ensign-Bickford Corporation, is laid across the loops and detonated at the far end. With a well-characterized detonation speed of $7 \text{ mm}/\mu\text{s}$, we expected it to provide a clean simulation of an actual shock wave. Figure 7 shows the result of a test on a six-loop sensor. Although six transitions clearly exist in this record of

detector output vs. time, the trend is not monotonically decreasing. Breaking certain fiber loops actually caused an increase in the demodulated signal, despite the loss of their contribution to the total. This seemingly bizarre behavior repeated itself on another similar experiment. We then performed the experiment using a steady laser-diode source at the same optical wavelength ($\sim 800 \text{ nm}$); the results are recorded in Figure 8. This record does exhibit the expected staircase pattern, which was also reproducible. Finally, we tested a 100-loop sensor, using a steady source. The record in Figure 9 demonstrates that the full sensor worked as expected; it consists of 100 downward steps, each small enough that the entire trace can be considered quasi-continuous. As we verified with the detonation cord alone, the initial dip and recovery were not related to the sensor itself, but were caused by EMP from the detonator circuit coupling into the detection electronics.

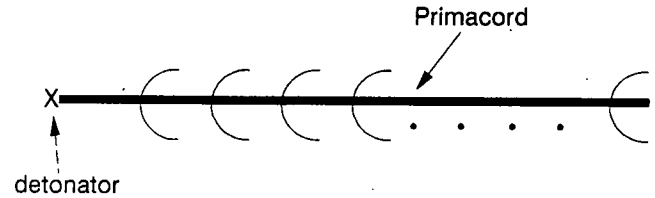


Figure 6. Explosives test arrangement for multiloop sensor

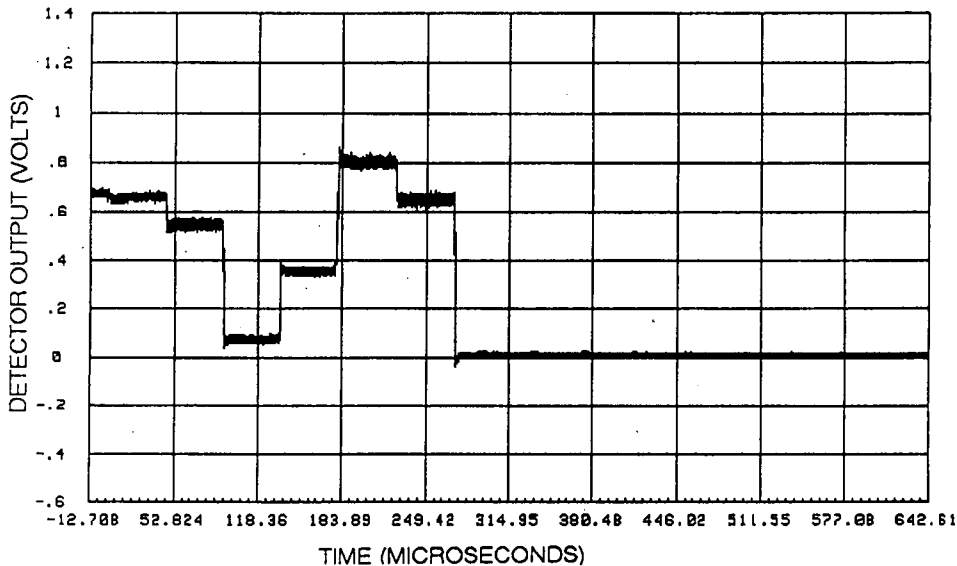


Figure 7. Six-loop sensor using modulated optical source

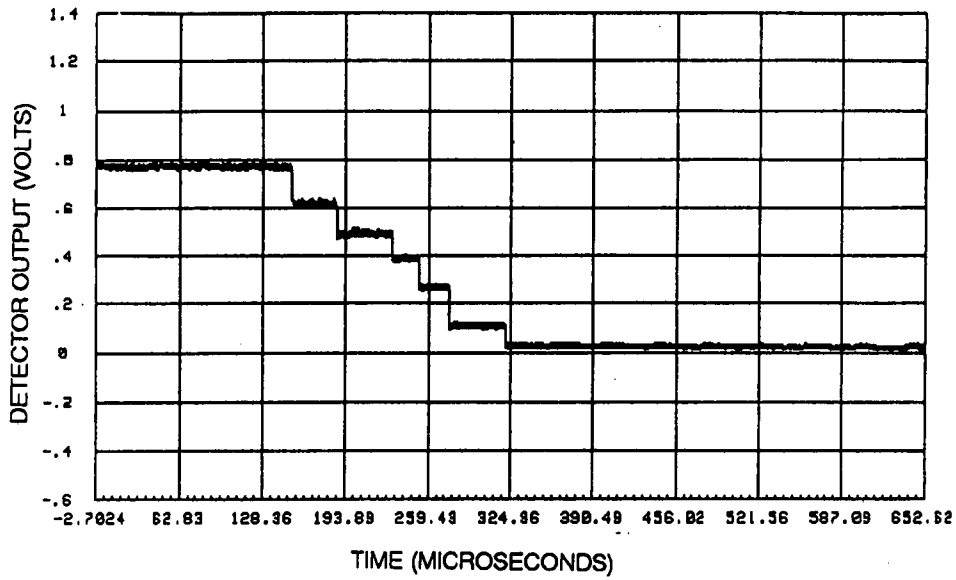


Figure 8. Six-loop sensor using steady optical source. Note that the spacing between loops is not uniform.

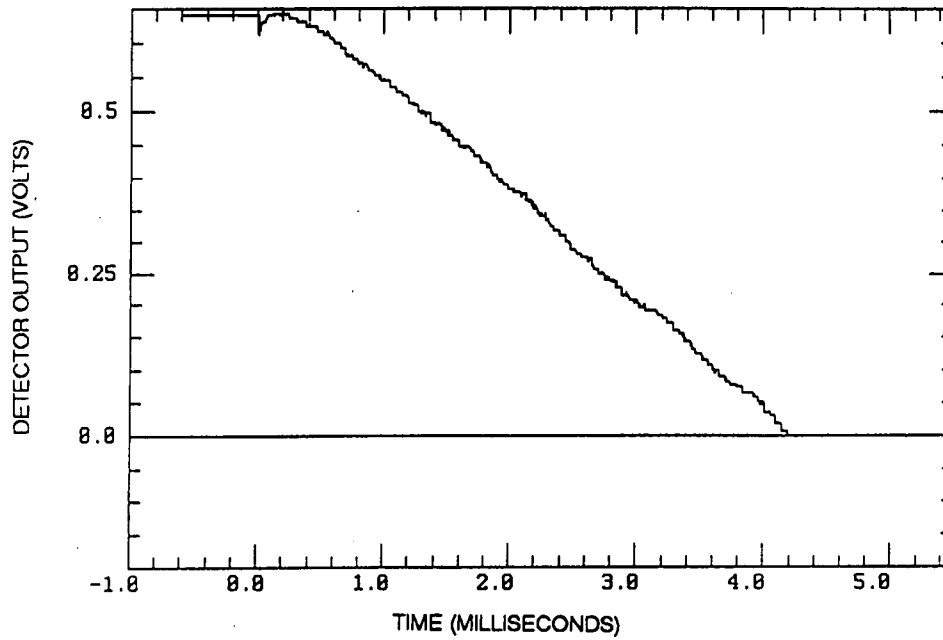


Figure 9. One hundred-loop sensor using steady optical source

Intensity Interferometric Sensor

We statically verified the nonmonotonic behavior of the six-loop sensor, excited by a modulated source, by manually making and unmaking various connections from one 1×6 fiber-optic coupler to another. Depending on where in a sequence a given connection was made, it either enhanced or diminished the amplitude of the modulated signal. Excitation by a steady laser source produced no such effect. It quickly became obvious that, although this sensor is not interferometric in the usual sense, a kind of interferometry was taking place associated with the modulated intensity. The relevant wavelength is λ_m , such that

$$\lambda_m = c/nf_m, \quad (3)$$

where c is the speed of light, n is the refractive index of the fiber, and f_m is the modulation frequency of the optical source. For a modulation frequency of 80 mHz, this wavelength is about 2.57 meters. Thus, depending on whether the phase of the modulated signal associated with a given connection is or is not within 90° of the phase of the total signal, due to all previous connections, it will either add to or subtract from that signal. That phase relationship is determined by the number of fibers that were connected previously and their lengths.

This intensity interferometry suggested an extremely simple kind of shock position sensor, as illustrated in Figure 10. Here, an optical fiber of length L is attached to a 1×2 coupler through a connector such that light reflects off this junction between the two fibers as well as at the far end of the fiber. These two reflections are in essence two sources of light, and whether they combine to produce an intensity maximum depends upon their phase difference at the connector. Obviously, if the round trip through the fiber is some integral multiple of λ_m , they will. Therefore, the change in the length of the fiber between successive maximums or minimums is $\lambda_m/2$, or about 1.29 meters for an 80-mHz signal. Higher modulation frequencies will diminish that number proportionately, and thereby increase the spatial resolution of this sensor.

Under shock conditions, the situation is not as clean as this analysis indicates, because the unpredictable character of the fiber end may cause a relatively poor reflection to occur just at the point of an interference maximum. Missing or shifted orders might then occur. This varying end-reflection is observed in Figure 11, which is the result of placing a length of detonation cord along the fiber in Figure 10 and initiating it. The optical source was unmodulated and the fiber end was initially polished, resulting in the best possible air-glass reflection (~4%) occurring before initiation. This is the level at the left of the figure. Thereafter, the reflection is almost always lower, and varies erratically until the cord has been completely consumed. The lowest level obtained during detonation corresponds to no reflection off the fiber end; this was determined by dipping it in index-matching gel and observing the detector output.

Despite the caveats associated with this technique, we demonstrated its viability by conducting the same experiment on an identical fiber (a 200- μ m core step-index fiber from Raychem Corp.) using an 80-mHz modulated source. We then performed the experiment again, this time using a 100- μ m core graded-index fiber from Corning, though this fiber end was initially dipped in index-matching gel. The results are shown in Figure 12a and b for the Raychem and Corning fibers, respectively. In contrast to Figure 11, we observe a definite periodicity in both cases, though as a consequence of the end effect just mentioned, it is not clearly sinusoidal. Furthermore, in the case of the Raychem fiber, the interference minimums are far more distinct than the maximums. Nevertheless, we can readily see that these extremes have the significance we have postulated for them, by noting that in both cases essentially 3.5 intervals between minimums occur within 0.655 millisecond. Dividing the time per interval into 1.29 meters results in a shock speed of 6.9 mm/ μ s; this is in excellent agreement with the nominal value of 7 mm/ μ s for the Primacord.

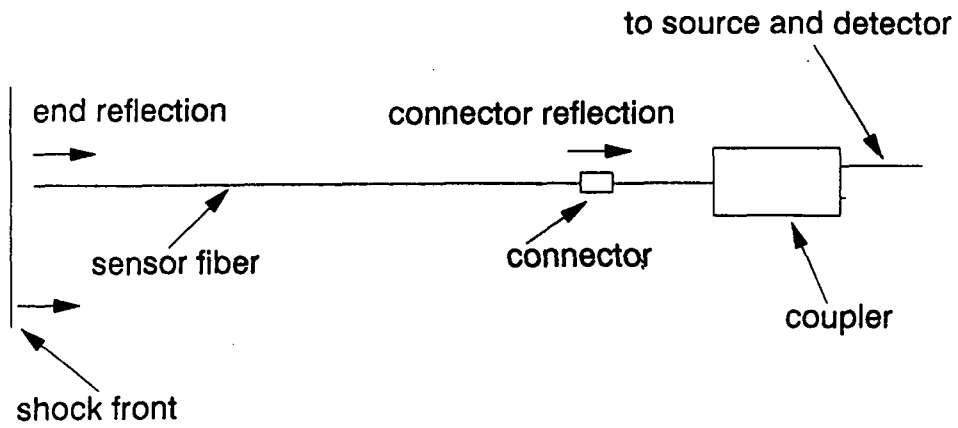


Figure 10. Intensity interferometric sensor

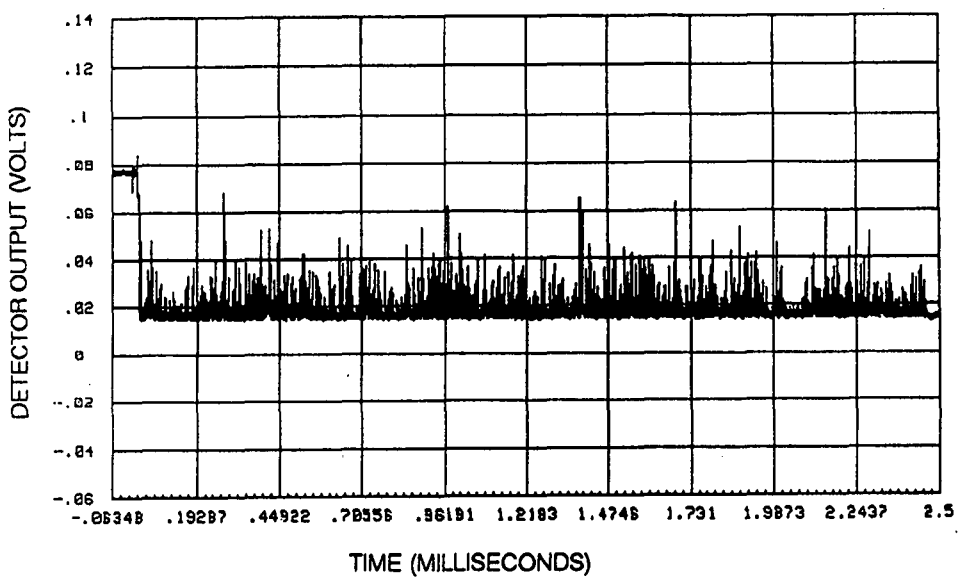
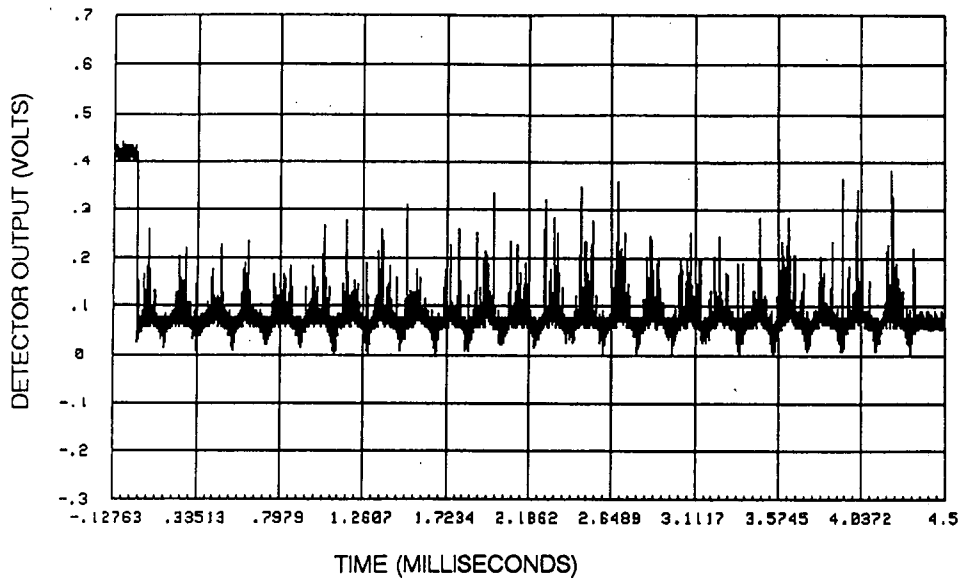
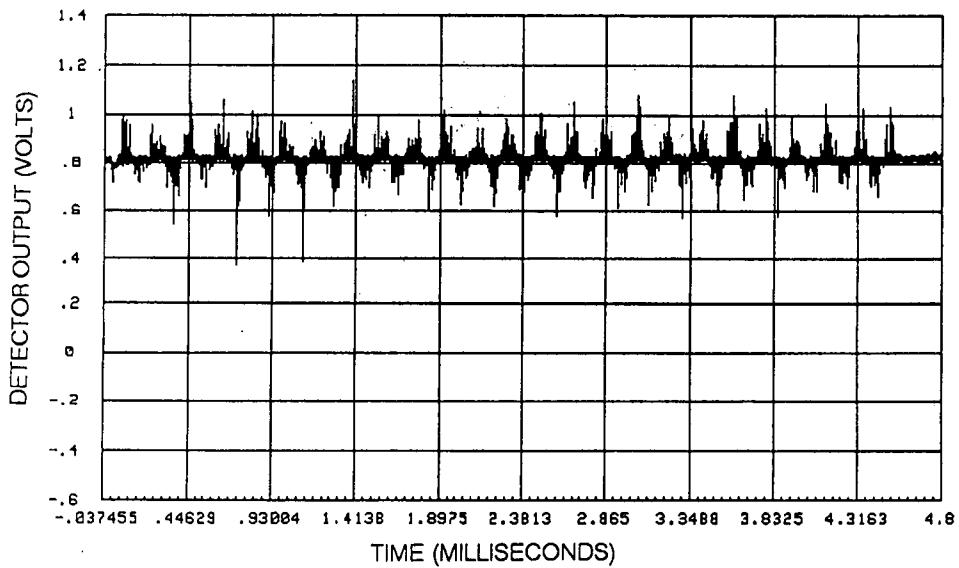


Figure 11. End reflections using a steady optical source (200 μ core, step-index fiber)



(a) 200 μ core, step-index fiber



(b) 100 μ core, graded-index fiber

Figure 12. End reflections using a modulated optical source

Embedded Grating Sensor

As part of this work, we explored another concept for a fiber-optic shock position sensor, though we never developed it. The basic configuration of such a device is shown in Figure 13, where an optical fiber contains reflection planes distributed in a known manner along its length. Ignoring all other reflections within the system, the totality of these reflectors determines the return signal. As the shock front proceeds, it destroys one reflector after another, thereby producing a staircase response similar to that in Figure 3.

As in the original proposal, this one does not depend on any lack of multiple reflections within the fiber, for such will exist. However, the composite reflectivity of the entire array can be analyzed, as we now show. Consider the first two reflection planes, with a distance between them much greater than the coherence length of the light source, having "elemental" intensity reflectivities r_1 and r_2 (Figure 14). Then by adding up the intensities of all the internal reflections, the overall reflectivity, R_2 , of the composite is shown to be:

$$R_2 = r_1 + r_2(1 - r_1)^2/(1 - r_1r_2) . \quad (4)$$

If we add a third reflection plane, having an elemental reflectivity r_3 , then the new composite reflectivity is:

$$R_3 = R_2 + r_3(1 - R_2)^2/(1 - R_2r_3) . \quad (5)$$

Generalizing to a composite consisting of n reflection planes:

$$R_n = R_{n-1} + r_n(1 - R_{n-1})^2/(1 - R_{n-1}r_n) . \quad (6)$$

For a constant r , we expect the multilayer reflectivity to asymptotically approach unity as the number of surfaces approaches infinity, implying a step size that approaches zero. If it is desired that the step size be a constant K , then $R_m = Km$, and r_m must vary. After solving Eq. (6) for r_m we obtain:

$$r_{m+1} = K/[(1 - Km)^2 + K^2m] . \quad (7)$$

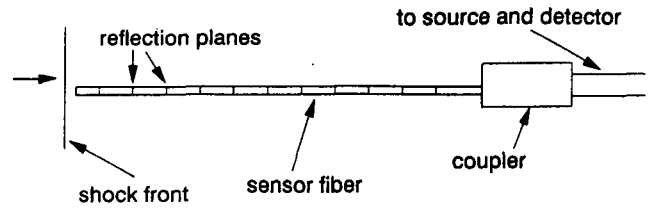


Figure 13. Embedded grating sensor

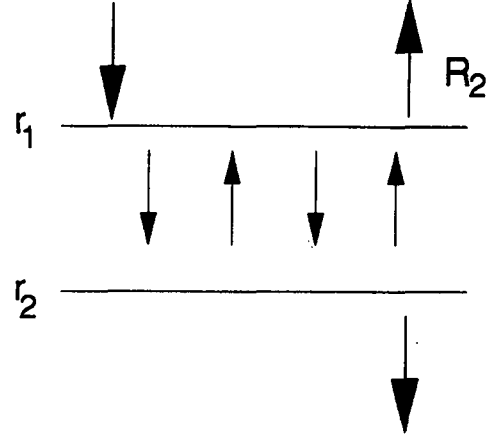


Figure 14. Two-surface reflection

We have calculated various cases of interest based on these equations. Figure 15 contains plots of the composite reflectivity vs. number of surfaces for a 100-surface sensor having all $r_m = 0.1$ and all $r_m = 0.01$. As expected, the step size is not constant, but diminishes as the number of surfaces increases. A trade-off clearly exists between range and sensitivity, where sensitivity is defined as the step size. Figure 16 consists of plots of the elemental reflectivity of a given surface vs. surface number for a 100-surface composite reflector whose composite reflectivity is 0.5 or 0.75 before exposure to a shock wave. Thus, $R_{100} = 0.5$ and $K = 0.005$, or $R_{100} = 0.75$ and $K = 0.0075$. It is interesting to note that one can produce a substantial composite reflectivity, as in the case of $R_{100} = 0.5$, without requiring any of the elemental reflectivities to exceed 2%.

We do not propose that these reflectors be actual mirrored surfaces between fiber segments, because such a device would be extremely tedious to fabricate and would probably result in considerable optical loss. Rather, we suggest that the reflection surfaces be periodic refractive-index distributions (or gratings) that have been “written” or embedded in the fiber. As in the case of any stratified medium, their reflectivity will depend upon the depth and spatial period of the modulation and the number of periods. The process of embedding these gratings would not involve any breaks in the fiber, but would be the same as that used by the United Technologies Research Corporation (UTRC) to create distributed fiber-optic sensors for “smart skin” applications.

When a germanium-doped optical fiber is exposed to ultraviolet radiation of about 240 nm, a photochemical change takes place that induces a corresponding change in the glass’ refractive index. A change as high as 0.006 has been reported by certain British researchers, but at UTRC 5×10^{-4} is typical.³ This refractive index change can be made periodic by introducing the ultraviolet radiation into the fiber as a standing-wave pattern. The spatial period that

optimizes reflection is $\lambda/2n$, where λ is the vacuum wavelength of the light reflected off the grating and n is the refractive index of the fiber. If we apply the theory of periodically stratified media⁴ as a reasonable description of a UTRC grating, then a 1% reflection can be achieved with a grating length of about 1500 such periods. This length is 0.4 mm for 800-nm light. Although not microscopic in thickness, it is still much thinner than the separation of at least several centimeters between gratings. It is thus thin enough to be considered a “surface” in the present context.

We should emphasize that the manufacturer of this sensor need not consult Figure 16, which was intended solely for illustrative purposes. Once an overall composite reflectivity is decided upon, a given step size could be achieved by monitoring the reflected light during the fiber’s exposure to the ultraviolet radiation. Exposure of that portion of the fiber will cease when the desired step size is achieved. The process would then be repeated down the line. Unfortunately, a lack of resources prevented us from pursuing the actual fabrication of this sensor.

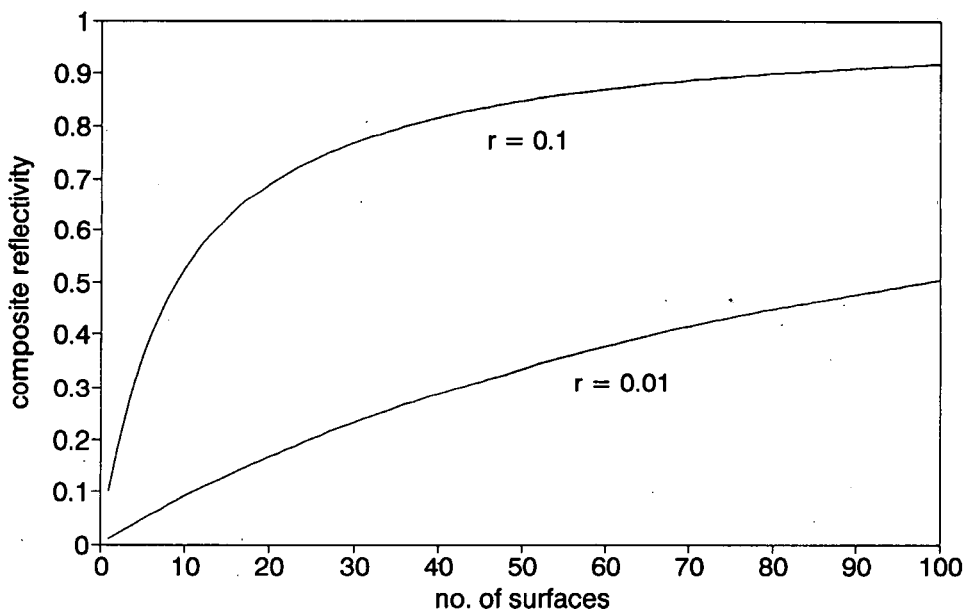


Figure 15. Composite reflectivity

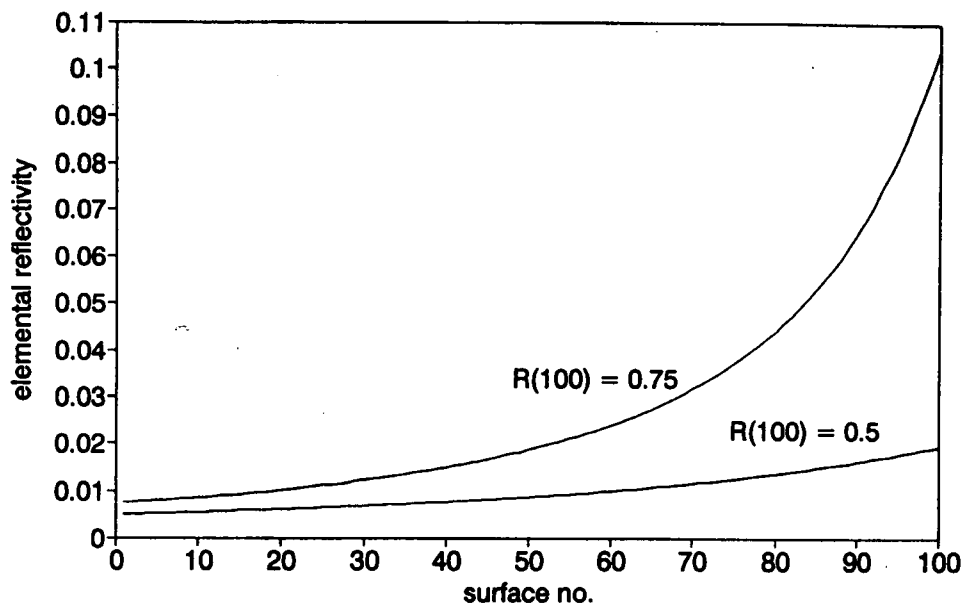


Figure 16. Elemental reflectivity

References

¹R. C. Bass and E. L. Larsen, *Shock Propagation in Several Geologic Materials in Hydrodynamic Yield Determinations*, SAND77-0402, Sandia Laboratories, Albuquerque, NM, 1977.

²Dimensions were obtained from the *Protocol to the Treaty Between the United States of America and the*

Union of Soviet Socialist Republics on the Limitation of Underground Nuclear Weapon Tests.

³William Morey, United Technologies Research Corporation, private communication with the author, January 1993.

⁴M. Born and E. Wolf, *Principles of Optics*, 5th edition, Section 1.6.5, Pergamon Press, 1975.

DISTRIBUTION:

1	Defense Nuclear Agency Attn: Mr. William J. Summa, FCTT Chief, Test Sci. & Tech. Office Field Command Kirtland AFB, NM 87117-5000	1	1000	L. M. Lopez
		1	1307	J. J. Wiczer
		1	2231	E. P. Royer
		1	2235	P. V. Dressendorfer
		1	4000	C. P. Robinson
		1	9000	G. Yonas
1	Defense Nuclear Agency Attn: Dr. George Lu Chief, Nevada Test Verification Div. PO Box 98539 Las Vegas, NV 89193	1	9300	J. E. Powell
		1	9301	J. D. Plimpton
		1	9305	M. J. Navratil
		1	9305	S. E. Dains
		1	9307	L. M. Choate
		1	9308	S. R. Dolce
1	Defense Nuclear Agency Attn: Mr Edward Martinez, TDTT Test Directorate Kirtland AFB, NM 87115	1	9311	A. J. Chabai
		1	9311	J. Banister
		1	9311	S. P. Breeze
		1	9312	K. M. Glibert
1	Defense Nuclear Agency Attn: Mr. Mark Flohr Code DFTR 6801 Telegraph Rd. Alexandria, VA 22310-3398	1	9312	G. J. Lockwood
		1	9312	S. S. Lopez
		15	9312	J. D. Weiss
		1	9321	W. B. Boyer
		1	8523-2	Central Technical Files
		5	7141	Technical Library
1	Mr. Norman Feder Canada Wire & Cable, Ltd. Canstar Division 3900 Victoria Park Ave. North York, Ontario CANADA M2H 3H7	1	7151	Technical Publications
		10	7613-2	Document Processing for DOE/OSTI